21 Jan 2013

A Novel Approach to Detecting Breathing-Fatigue Cracks based on Dynamic Characteristics

Guirong Yan
Missouri University of Science and Technology, yang@mst.edu

Alessandro De Stefano

Emiliano Matta

Ruoqiang Feng

Recommended Citation

G. Yan et al., "A Novel Approach to Detecting Breathing-Fatigue Cracks based on Dynamic Characteristics," *Journal of Sound and Vibration*, vol. 332, no. 2, pp. 407 - 422, Elsevier, Jan 2013.
The definitive version is available at https://doi.org/10.1016/j.jsv.2012.09.008

Journal of Sound and Vibration 332 (2013) 407–422

Contents lists available at SciVerse ScienceDirect

Journal of Sound and Vibration

journal homepage: www.elsevier.com/locate/jsvi

A novel approach to detecting breathing-fatigue cracks based on dynamic characteristics

Guirong Yan [a,b,*], Alessandro De Stefano [b], Emiliano Matta [b], Ruoqiang Feng [c]

[a] Department of Civil Engineering, University of Texas at El Paso, El Paso, TX 79968, USA
[b] Department of Structural and Geotechnical Engineering, Polytechnic Institute of Turin, Turin 10029, Italy
[c] The Key Laboratory of Concrete and Prestressed Concrete Structures of Ministry of Education, Southeast University, Nanjing, Jiangsu Province 210096, People s Republic of China

ARTICLE INFO

Article history:
Received 1 October 2011
Received in revised form
22 May 2012
Accepted 7 September 2012
Handling Editor: I. Trendafilova
Available online 1 October 2012

ABSTRACT

During the service life of structures, breathing-fatigue cracks may occur in structural members due to dynamic loadings acting on them. These fatigue cracks, if undetected, might lead to a catastrophic failure of the whole structural system. Although a number of approaches have been proposed to detect breathing-fatigue cracks, some of them appear rather sophisticated or expensive (requiring complicated equipment), and others suffer from a lack of sensitivity. In this study, a simple and efficient approach to detecting breathing-fatigue cracks is developed based on dynamic characteristics of breathing cracks. First, considering that breathing cracks introduce bilinearity into structures, a simple system identification method for bilinear systems is proposed by taking best advantage of dynamic characteristics of bilinear systems. This method transfers nonlinear system identification into linear system identification by dividing impulse or free-vibration responses into different parts corresponding to each stiffness region according to the stiffness interface. In this way, the natural frequency of each region can be identified using any modal identification approach applicable to linear systems. Second, the procedure for identifying the existence of breathing fatigue cracks and quantifying the cracks qualitatively is proposed by looking for the difference in the identified natural frequency between regions. Third, through introducing Hilbert transform, the proposed procedure is extended to identify fatigue cracks in piecewise-nonlinear systems. The proposed system identification method and crack detection procedure have been successfully validated by numerical simulations and experimental tests.

1. Introduction

During the service life of structures, fatigue cracks may occur in structural members due to dynamic loadings acting on them. If the static deflection due to such loadings as dead loads is smaller than the vibration amplitude caused by dynamic loadings, these fatigue cracks alternately open and close with time [1], exhibiting a breathing-like behavior. Various theoretical and experimental studies have shown that breathing-fatigue cracks cause smaller changes in dynamic characteristics than open cracks with the same size, and thus are more difficult to be detected. Fatigue cracks, if

* Corresponding author at: School of Engineering, University of Western Sydney, Penrith, 2750 NSW, Australia. Tel.: +61 2 4736 0641.
E-mail addresses: ygr1975@126.com, g.yan@uws.edu.au (G. Yan).

0022-460X/$ - see front matter © 2012 Elsevier Ltd. All rights reserved.
http://dx.doi.org/10.1016/j.jsv.2012.09.008

undetected, might lead to a catastrophic failure of the whole structural system [2–4]. Therefore, the detection of fatigue cracks has been extensively studied since the 1940s and a number of methods have been proposed.

Local detection methods using lamb waves [5,6] and laser ultrasound [7] as well as acoustic emission techniques [8] have been explored to detect fatigue cracks. These methods have been proven to be accurate. However, they typically require either a long-time inspection process due to a small inspection area at one time or a temporary interruption of operational conditions for carrying out inspections. To overcome these disadvantages, crack detection based on nonlinear dynamic behaviors of breathing-fatigue cracks has been actively studied. For example, Tsyfansky and Beresnevich [9] identified fatigue cracks in flexible, geometrically nonlinear beams using the presence of super harmonic components in responses; Bovsunovskya and Surace [10] took both sub- and superharmonic resonances of responses as indicators of the presence of a crack; Leonard et al. [11] employed the frequency spectrogram and a criterion based on the coherent power of amplitude modulation to detect fatigue cracks in a cantilever beam; Rivola and White [12] detected the existence of a fatigue crack by means of bispectral analysis, which was a subset of higher-order statistical analysis; Surace et al. [13] applied higher order Frequency Response Functions (FRFs) which are based on the Volterra series to detect cracks in beam-like structures; Loutridis et al. [14] proposed a crack identification method based on the instantaneous frequency which was obtained by performing Hilbert transform on the obtained modes using the empirical mode decomposition of responses. Ryue and White [15] investigated the feasibility of attractor-based measurements under a chaotic excitation to detect cracks in a structure.

Due to the breathing behavior of fatigue cracks, the system stiffness changes at the instant of crack opening and closing, and thus the system with breathing-fatigue cracks exhibits bilinear stiffness characteristics. This has been validated by Gudmundson [16] using experimental tests and validated by Ibrahim using numerical analysis [17]. However, the system with breathing cracks, as a bilinear system, behaves linearly in each stiffness region. In this study, a simple and efficient approach to detecting breathing-fatigue cracks is developed based on dynamic characteristics of systems with fatigue cracks. First, considering the linear characteristic in each stiffness region and the bilinear characteristic in the whole system, a simple system identification method for bilinear systems is proposed. The central idea of the proposed method is as follows: the responses associated with different stiffness regions are first separated from one another, and then the natural frequencies in each region can be identified from the respective separated responses using any approach proposed for linear systems. In this way, the problem of nonlinear system identification is transferred into that of linear system identification. Second, by looking for the difference in the identified natural frequency between stiffness regions, the fatigue crack can be directly identified and further quantified when the damage location is known.

This paper is organized as follows. In Section 2, a system identification method for bilinear systems is proposed. In Section 3, how to apply the identified parameters to detect fatigue cracks is discussed, and the procedure for identifying the existence of breathing cracks and quantifying the cracks qualitatively is developed. Section 4 presents how to extend the proposed procedure to identify breathing cracks in piecewise-nonlinear systems. In Sections 5 and 6, the performance of the proposed method and procedure is demonstrated by numerical simulations and experimental tests, respectively.

2. A system identification method for bilinear systems through separating global responses

In this section, dynamic characteristics of bilinear systems are first studied. Then, a system identification method is proposed for bilinear systems by separating the impulse or free-vibration responses at the stiffness interface. This method takes best advantage of dynamic characteristics of bilinear systems.

2.1. Dynamic characteristics of bilinear systems

Consider a Single-Degree-Of-Freedom (SDOF) bilinear system in which the change in stiffness occurs at its static equilibrium position $x=0$, as shown in Fig. 1. Physically, each time the oscillator crosses the interface between the two stiffness regions ($x=0$), the stiffness of the system changes. The equation of motion of the system under free vibration can

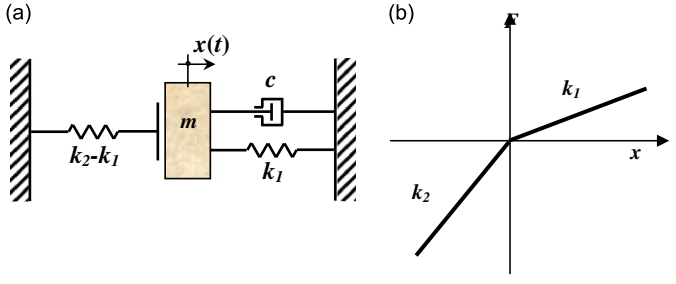

Fig. 1. Physical model and stiffness characteristic of a bilinear oscillator: (a) physical model of a bilinear oscillator and (b) restoring force model of the bilinear oscillator.

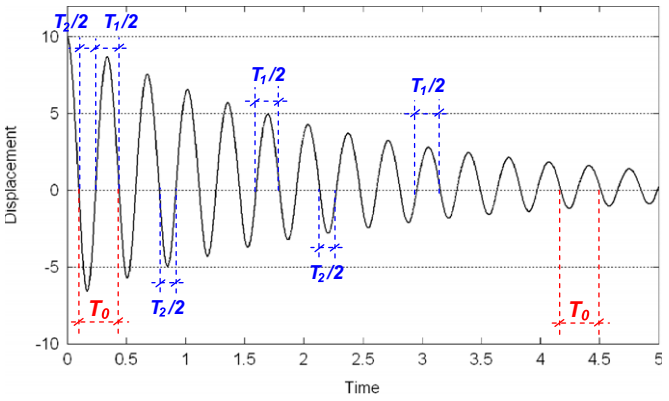

Fig. 2. Displacement responses under free vibration of the bilinear oscillator. *Note*: T_1 and T_2 represent the oscillation periods corresponding to the two regions, respectively.

be described as

$$\begin{cases} m\ddot{x}+c_1\dot{x}+k_1x=0, & x\geq 0 \quad (a) \\ m\ddot{x}+c_2\dot{x}+k_2x=0, & x<0 \quad (b) \end{cases} \tag{1}$$

where x is the displacement of the bilinear oscillator; m and c are its mass and damping coefficients, respectively; k_1 and k_2 are the stiffness coefficients in the two stiffness regions.

Nondimensionalizing Eq. (1) with mass m yields

$$\ddot{x}+2\xi_1\omega_1\dot{x}+\omega_1^2x=0, \quad x\geq 0 \tag{2a}$$

$$\ddot{x}+2\xi_2\omega_2\dot{x}+\omega_2^2x=0, \quad x<0 \tag{2b}$$

where ω_1 and ω_2 denote the circular frequencies of each stiffness region, respectively. Herein $\omega_1<\omega_2$. ξ_1 and ξ_2 are the modal damping ratios of each stiffness region.

Free-vibration responses of this bilinear oscillator can be obtained by solving Eq. (2a) and Eq. (2b) for responses in each of the two stiffness regions, and matching the responses in the two regions through the continuity of both displacement and velocity at the stiffness interface [3,18].

Fig. 2 presents the free-vibration responses of the bilinear oscillator. From this figure, the free-vibration responses are periodical and the vibration period during the whole vibration duration keeps constant, designated T_0. It seems that the vibration period (and accordingly, the vibration frequency) of a bilinear system does not vary with time or amplitude, unlike other nonlinear systems. The vibration period T_0 and vibration frequency ω_0 can be expressed as [3]

$$T_0=\frac{T_1}{2}+\frac{T_2}{2} \quad \text{where } T_1=\frac{2\pi}{\omega_1} \text{ and } T_2=\frac{2\pi}{\omega_2} \tag{3}$$

$$\omega_0=\frac{2\pi}{T_0}=\frac{2\omega_1\omega_2}{\omega_1+\omega_2} \tag{4}$$

Here, ω_0 is called the bilinear frequency [3], which represents the free-vibration frequency of the bilinear oscillator and satisfies $\omega_1<\omega_0<\omega_2$. Eq. (4) holds rigorously true only for an undamped system. For a damped system, ω_1 and ω_2 should be replaced by the damped circular frequencies of each region. However, because the damping ratio is usually small in practice, Eq. (4) still holds true for a damped system.

Based on the above observation, Fourier transform is applicable to the global free-vibration responses. The peaks in the auto power spectral density (PSD) of the global responses correspond to the bilinear frequency ω_0 and its higher harmonics which are caused by the presence of stiffness bilinearity. However, the natural frequency of each region cannot be obtained from ω_0, i.e., directly extracting the natural frequency of each region from the global responses does not seem possible. This motivates the present attempt to identify the natural frequencies of both regions from their respective local responses, as is explained below.

From Fig. 2, although the vibration period of the system obtained from the global responses does not vary with time, the time durations of the two half-sine waves in each period ($T_1/2$ and $T_2/2$, respectively) are different (to be exact, $T_1/2>T_2/2$, which is consistent with $\omega_1<\omega_2$). However, the time durations of all of the half-sine waves in the upper region (*displacement* ≥ 0) are exactly the same and it is the same case for all of the half-sine waves in the lower region (*displacement* <0). This suggests that although the system exhibits a nonlinear behavior in each entire vibration period, it still behaves linearly in each stiffness region. This can be easily understood by reconsidering Eq. (1). Actually, all positive responses are calculated from Eq. (1a) and all negative ones are calculated from Eq. (1b), and global responses are obtained by matching the two parts of local responses at the stiffness interface (*displacement*$=0$).

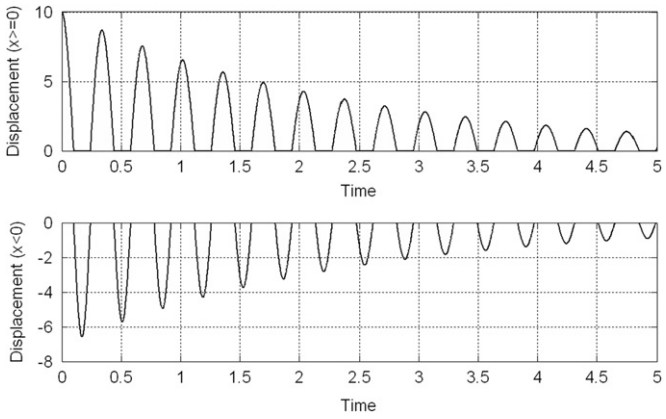

Fig. 3. Separation of global responses into two parts at the stiffness interface (*displacement*=0).

2.2. Identification of natural frequency in each region

Based on the above analysis, positive responses only include information on the parameters of the stiffness region $x \geq 0$ (parameters in Eq. (1a)), and negative responses only include information on the parameters of the stiffness region $x < 0$ (parameters in Eq. (1b)). If the parameters of the region $x \geq 0$ are to be determined, only the positive responses are needed, and vice versa. Based on this observation, a novel, simple method is proposed to identify the modal parameters of each region.

First, the measured global impulse or free-vibration responses are divided into two parts at the stiffness interface (*displacement*=0). Fig. 3 presents the separated responses above and below the axis of *displacement*=0. This simulates that only a half-sine wave in each vibration period is acquired during measurement.

Then, the half-sine waves in each region are assembled together so as to reconstruct a signal in which only the half-sine waves in the respective region are involved (the black graph in Fig. 4). In this paper, the assembled signal is called the local responses corresponding to each region, "local responses" for short. Because the period of the half-sine wave in each set of local responses does not vary with time, Fourier transform or any other linear modal identification approach can be applied to identify modal parameters in the respective region. System parameters associated with the region $x \geq 0$ can be extracted from the local responses in the upper region (above the axis of *displacement*=0), and the system parameters associated with the region $x < 0$ can be extracted from the local responses in the lower region (below the axis of *displacement*=0). By separating global responses into two parts, the problem of nonlinear system identification is transferred to that of linear system identification. Actually, the frequency obtained from this assembled signal is twice the natural frequency of the associated region, and some higher harmonic components may occur.

To get the correct natural frequency of the associated region, an extra procedure may be performed on each set of local response data. That is, every second half-sine wave is inverted to form entire sine waves (the red dashed graph in Fig. 4). Actually, this procedure generates a signal representing the responses of a linear system which has the same natural frequency as the system in each region, but has a different damping ratio from the system in each region, which can be reflected by the difference between the graph with the mark of "x" and the one with the mark of "o", as shown in Fig. 4. The identification of the damping ratio in each region is to be discussed in another paper. Compared with the nonlinear system identification methods reviewed by Farrar et al. in Ref. [19], the proposed method is much simpler.

3. Crack detection by comparing identified natural frequencies in two stiffness regions

In this section, the procedure for identifying the presence of fatigue cracks and quantifying the cracks qualitatively is developed based on the system identification results using the method proposed in Section 2.

A cantilever beam containing a breathing crack (shown in Fig. 5) is considered to illustrate the proposed procedure. When the beam moves downwards, the upper fibers are stretched and the crack opens; when the beam moves upwards, the upper fibers are compressed and the crack closes. The stiffness coefficient of the system varies during vibration. Therefore, this beam is a bilinear system.

Recall that vibration responses of a structure can be taken as the superimposition of weighted mode shapes and under each mode the structure can be taken as an SDOF system [20]. Therefore, if the beam vibrates under a specific mode, it can be simulated as an oscillator with bilinear stiffness [24]. Assuming that the crack is fully opened and closed during vibration and the crack does not change the mass and damping of the system, the equation of motion of the cracked beam under each mode can be expressed as Eq. (1) or (2). Here the mass and stiffness coefficients should be the generalized mass and stiffness for the specified mode [24].

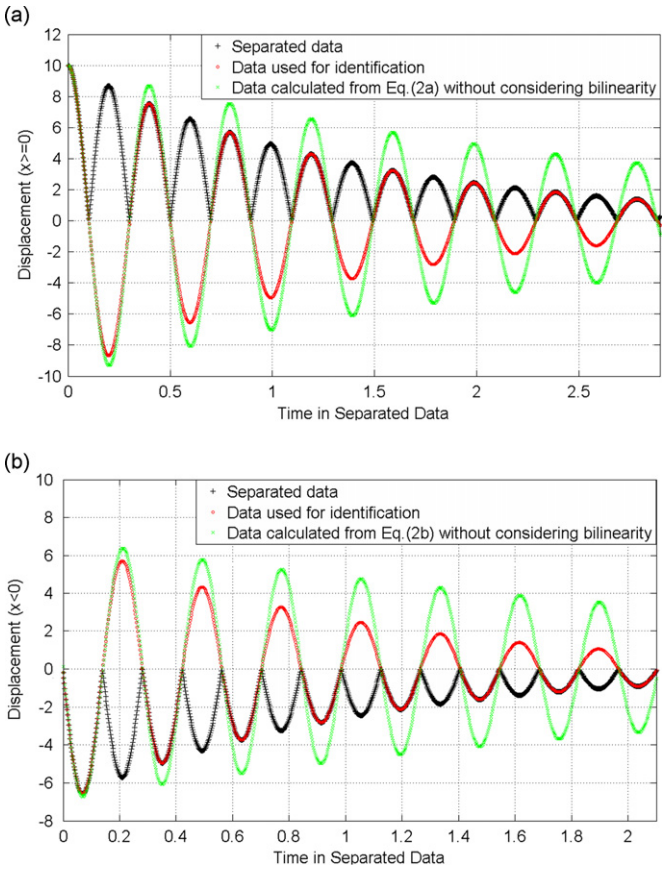

Fig. 4. Generation of local response data for system identification: (a) response data in region $x \geq 0$ and (b) response data in region $x < 0$. (For interpretation of the references to color in this figure legend, the reader is referred to the web version of this article.)

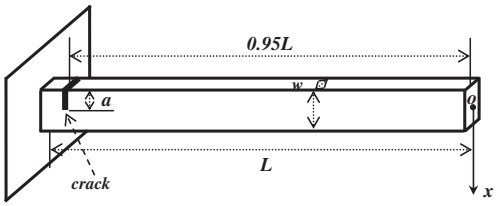

Fig. 5. A cantilever beam with a breathing crack.

In particular, k_1 and k_2 denote the generalized stiffness coefficients when the crack opens and closes, respectively. Accordingly, ω_1 and ω_2 represent the system circular frequencies of the two stiffness regions. k_2 is exactly the same as the stiffness coefficient of the associated uncracked beam. Assuming that the crack introduces a local flexibility, k_1 can be obtained by Fracture Mechanics. k_1 changes with the size and location of the crack. More details about obtaining k_1 and k_2 will be introduced in Section 5.2.

Each time the beam vibration crosses the undeformed point ($x=0$), the system stiffness changes, and thus the natural frequency in each region changes accordingly. The natural frequency in each region can be identified from the corresponding set of local responses separated from global responses, as proposed in Section 2. By looking for the difference in the natural frequencies extracted from the two regions, one can tell whether a breathing crack occurs or not. If the beam is not cracked, the difference will be zero. If a breathing crack occurs, the natural frequency of one region will deviate from that of the other region.

In addition, the size and location of the fatigue crack determine the stiffness k_1, affecting the natural frequency in the associated stiffness region and thus affecting the difference in natural frequencies between the two regions. Therefore, if the damage location is found, crack severity can be reflected from this difference. The procedure for detecting breathing cracks in a beam is summarized in Fig. 6. The crack identification and quantification could be obtained for

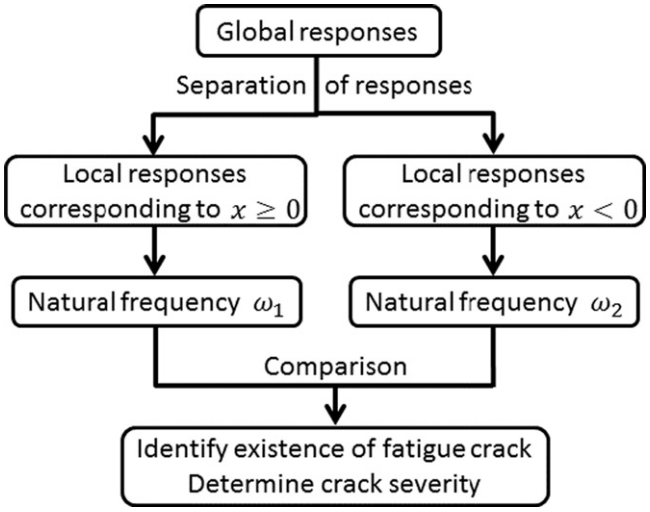

Fig. 6. Flowchart of detection of breathing cracks by comparing identified natural frequencies in two stiffness regions.

Multiple-Degree-of-Freedom systems, with only slight modifications of the proposed procedure, but this objective exceeds the scope of the present paper.

The procedure proposed in this paper for identifying and quantifying breathing cracks has the following three advantages:

(1) it does not require the baseline data (the responses measured from the intact beam). Only the responses in the current state are required to be measured;
(2) it avoids the influences of the differences in environmental factors (such as temperature and humidity), boundary conditions and/or measurement errors [21] before and after damage, because the local responses from which the natural frequency of each region is extracted are obtained by separating the same global responses measured in the current state. On the contrary, traditional approaches which compare the natural frequencies of structures (bilinear frequencies for systems with breathing cracks) before and after damage are often affected by the factors mentioned above. Therefore, the change in bilinear frequencies caused by these factors may be greater than that caused by damage.
(3) the proposed procedure (comparing the natural frequencies between the two regions) is more sensitive than traditional approaches (comparing the bilinear frequencies, ω_0, before and after damage, which are extracted from global responses). Even though a severe breathing crack occurs, the change in ω_0 may be very small. This is because the breathing crack just affects the responses and natural frequency in one region, and the bilinear frequency is extracted from the responses of both regions, which would underestimate the damage. To further demonstrate this, the sensitivity analysis is performed as follows.

Before a breathing crack occurs in a beam, the natural frequencies in the two regions are equal, i.e., $\omega_1 = \omega_2$ and their values are set to be ω, and thus the bilinear frequency can be computed using Eq. (4)

$$\omega_0 = \frac{2\omega_1\omega_2}{\omega_1+\omega_2} = \frac{2\omega\omega}{\omega+\omega} = \omega \tag{7}$$

Once a crack occurs and breathes during vibration, the natural frequency of the region $x \geq 0$ (ω_1) is reduced and it is assumed to be reduced to $\alpha\omega$, while ω_2 remains unchanged and is equal to ω. Accordingly, the breathing crack necessarily results in a change in the bilinear frequency. Suppose that ω_0 reduces to $\beta\omega$, which can be expressed in terms of the natural frequencies in the two regions using Eq. (4)

$$\beta\omega = \frac{2\alpha\omega\omega}{\alpha\omega+\omega} = \frac{2\alpha\omega}{1+\alpha} \tag{8}$$

Then, the change in the bilinear frequency before and after damage, $\Delta\omega_0$, can be obtained as

$$\Delta\omega_0 = (1-\beta)\omega = \omega - \frac{2\alpha\omega}{1+\alpha} = \frac{(1-\alpha)\omega}{1+\alpha} \tag{9}$$

where $(1-\alpha)\omega$ denotes the difference in natural frequency between the two regions, designated as $\Delta\omega$.

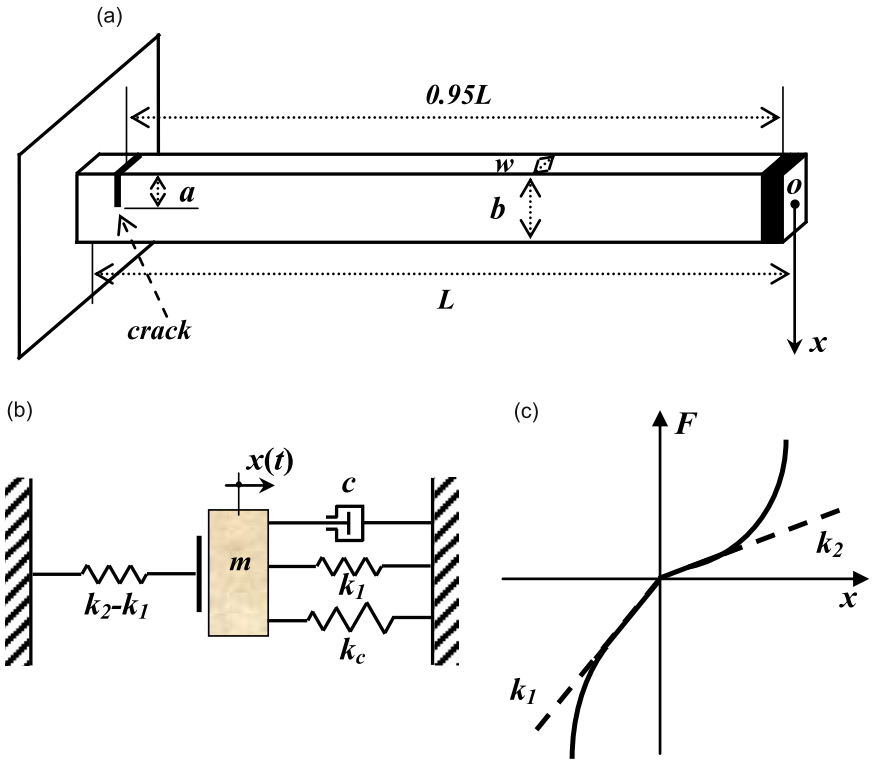

Fig. 7. A system with piecewise-nonlinearities and its stiffness characteristic: (a) cantilever beam with a large deflection, (b) simplified model of the cracked beam, and (c) restoring force model of the cracked beam.

The relationship between $\Delta\omega$ and $\Delta\omega_0$ can be obtained by rearranging Eq. (9)

$$\frac{\Delta\omega_0}{\Delta\omega}=\frac{(1-\beta)\omega}{(1-\alpha)\omega}=\frac{1}{1+\alpha} \tag{10}$$

where $0<\alpha<1$, and thus $\Delta\omega_0$ must be less than $\Delta\omega$, i.e., the change in the bilinear frequency is less sensitive to a breathing crack than the proposed procedure. Therefore, the severity of the crack will be underestimated by traditional approaches which are based on the bilinear frequency.

4. Crack detection for systems with piecewise-nonlinearities

The crack detection procedure proposed in Section 3 is applicable to systems which are linear in each stiffness region. For systems which are nonlinear in each stiffness region, an extended approach is developed by introducing Hilbert transform. The extended procedure is illustrated in this section using a cantilever beam with a large deflection (shown in Fig. 7(a)). This system possesses geometrical nonlinearity in its intact state, which can be simulated by cubic stiffness. If a breathing crack occurs in this beam, it cannot be modeled by a piecewise-linear system any more, but a piecewise-nonlinear system, as shown in Fig. 7(b) and (c).

To be exact, under a specific mode, the beam with a large deflection can be taken as an SDOF system with cubic stiffness nonlinearity. Accordingly, the cracked beam can be modeled as an SDOF system with both bilinear and cubic stiffness, as shown in Fig. 7(b) and (c). The governing equation of motion can be written as

$$\begin{cases} m\ddot{x}+c_1\dot{x}+k_1x+k_{c1}x^3=0, & x\geq 0 \\ m\ddot{x}+c_2\dot{x}+k_2x+k_{c2}x^3=0, & x<0 \end{cases} \tag{11}$$

where x is the displacement response; m is the system mass; c_1 and c_2 are the damping coefficients in the two regions, respectively; k_1 and k_2 are the linear stiffness coefficients in the two regions, respectively; k_{c1} and k_{c2} are the nonlinear stiffness coefficients. Nondimensionalizing Eq. (11) yields

$$\begin{cases} \ddot{x}+\frac{c_1}{m}\dot{x}+\omega_1^2x+\frac{k_{c1}}{m}x^3=0, & x\geq 0 \\ \ddot{x}+\frac{c_2}{m}\dot{x}+\omega_2^2x+\frac{k_{c2}}{m}x^3=0, & x<0 \end{cases} \tag{12}$$

where ω_1 and ω_2 are the circular frequencies of the underlying linear system in each region.

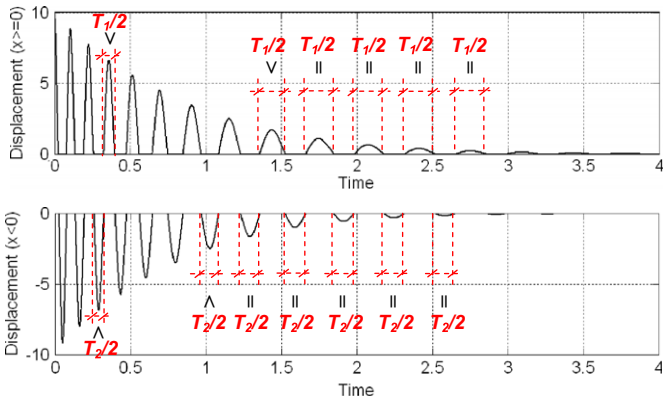

Fig. 8. Separation of global responses into two parts for a piecewise-nonlinear system.

Herein, the opening and closing of the fatigue crack during vibration result in the difference in linear stiffness between the two regions, which introduces bilinearity into the system, the same as in Section 3. However, in each region, the system is no longer linear, exhibiting cubic stiffness nonlinearity when the displacement response x is large enough. Therefore, the cracked beam exhibits the characteristics of both bilinearity and cubic nonlinearity at the same time.

Assuming that breathing cracks affect only the linear stiffness, the critical step for detecting breathing cracks is to identify the natural frequency of the underlying linear system in each region, ω_1 and ω_2. First, the local response data corresponding to each region is obtained by separating global responses into two parts at the stiffness interface, the same as in Section 2. The obtained local responses only include information on cubic nonlinearity.

Second, ω_1 and ω_2 are identified from the associated set of local response data. Because the system exhibits cubic stiffness nonlinearity in each stiffness region, ω_1 or ω_2 depends on the vibration amplitude [22]. In each region, the relationship between the instantaneous frequency (IF) and the instantaneous vibration amplitude (IVA) is as follows

$$\omega_I(t_i) = \omega_l + \frac{3A(t_i)^2}{8m}\frac{k_c}{\omega_l} \tag{13}$$

where ω_l is the circular frequency of the underlying linear system in each region, i.e., ω_1 or ω_2; $\omega_I(t_i)$ and $A(t_i)$ denote the IF and IVA at each sampling instant t_i in the associated region. For positively damped systems whose IVA decays with time, the characteristic of amplitude-dependency results in the variation of the IF with time, as shown in Fig. 8. Obviously, Fourier spectrum of the responses during the whole sampling duration in each region cannot accurately represent the dynamic characteristics of each region. On the contrary, the IF at each sampling instant can completely capture the dynamic characteristics of each region.

From Eq. (13), if $A(t_i)$ at the sampling instant t_i is sufficiently small, the influence of cubic nonlinearity is small enough to be negligible, and thus the $\omega_I(t_i)$ can be taken as the linear natural frequency in each region, ω_l [23]. Therefore, towards the end of the decaying vibration where the vibration amplitude $A(t_i)$ is small, the IF tends to be a constant and to be equal to the natural frequency of the underlying linear system in each region, i.e., $\omega_l = \omega_I(t_i)$. However, at the very end of the decaying vibration where $A(t_i)$ approaches to zero, the extracted IF may experience significant fluctuations due to a low signal-to-noise ratio. Therefore, the IFs associated with the very end of the vibration cannot be used as an estimate of the natural frequency of the underlying linear system. Herein, Hilbert transform is performed on each set of local response data to extract the IF of each region as follows:

(1) the corresponding analytic signal Y of the local response data y is obtained using Hilbert transform

$$Y = y + iH(y) \tag{14}$$

where $H(y)$ is Hilbert transform of the response data y.

(2) the IF at the sampling instant t_i can be obtained through differentiating the phase of Y with respect to time t as

$$\omega_I(t_i) = \left.\frac{d\psi_Y(t)}{dt}\right|_{t=t_i} \tag{15}$$

Third, the natural frequency of the underlying linear system in each region, ω_l, can be obtained by calculating the mean value of the IFs in the range towards the end of vibration.

Finally, by comparing the natural frequencies of the two regions, one can tell whether a breathing crack is occurring or not and how serious the crack is if the crack location is identified.

5. Numerical simulations

5.1. A bilinear oscillator

This example is to demonstrate the effectiveness of the proposed system identification method for bilinear systems. Consider a bilinear oscillator whose motion was governed by Eq. (1). The system parameters were chosen as $m=1$ kg, $k_2=3\times10^4$ N m^{-1}, and $k_1=\alpha k_2$. Here α represented the stiffness ratio and it is equal to 0.5 in this case. The natural frequencies in the regions $x\geq 0$ and $x<0$ were 19.49 Hz and 27.57 Hz, respectively. Assume that the damping ratios in the two regions were 0.14% and 0.20%, respectively.

A numerical algorithm based on a fourth-order Runge–Kutta integration scheme was employed to calculate acceleration responses. To simulate an impact excitation, the initial displacement was set to 0 and the initial velocity was set to 1 m/s. The response time history was assumed to be acquired at the sampling frequency of 512 Hz and the acquisition duration was 20 s. To investigate the effectiveness of the proposed method in the presence of measurement noises, Gaussian white noises with the mean value of zero and the RMS (root-mean-square) equal to 5% and 10% of that of responses were added to the obtained acceleration responses.

Fig. 9(a) plots the calculated acceleration response data. It is found that the response amplitudes are not symmetric about the axis of *displacement*=0, which is a time-domain distortion caused by bilinearity. In the auto power spectral density of global acceleration responses shown in Fig. 9(b), the peaks correspond to the bilinear frequency (23 Hz) and one higher harmonic component (46 Hz), which is the consequence of the presence of bilinearity.

To use the proposed method, the global acceleration responses were first separated into two parts, forming two sets of local response data. Positive acceleration responses correspond to the region $x<0$, and vice versa. This corresponding relationship exists because the phase difference between acceleration and displacement responses is π. Then, within each set of local response data, through finding the transition points whose slopes change signs, each second half-sine wave was inverted. For example, for the acceleration responses in the region $x<0$ (positive acceleration responses), the transition points were those whose slope signs change from $x<0$ to $x>0$. Third, the auto power spectral density associated with each region was obtained by performing Fourier transform on each set of local response data, as shown in Fig. 9(c) and (d).

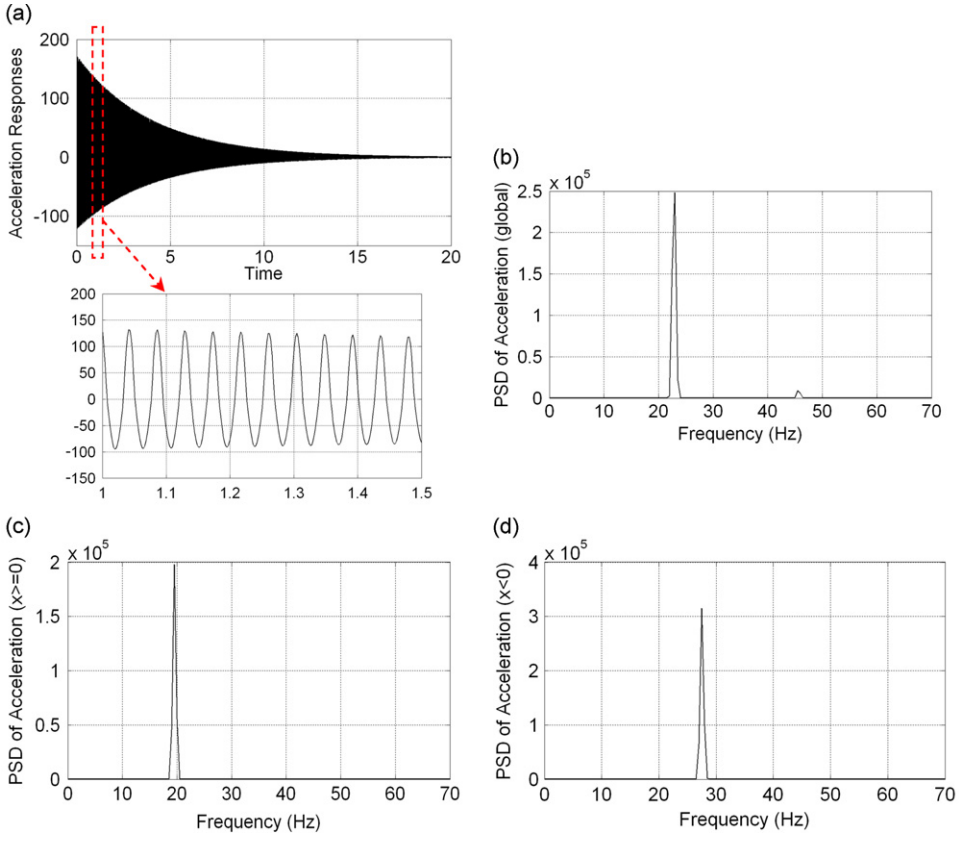

Fig. 9. Acceleration responses and auto power spectral density of global and local response data: (a) acceleration time history, (b) power spectral density of global responses, (c) power spectral density of local responses associated with the region $x\geq 0$, and (d) power spectral density of local responses associated with the region $x<0$.

Table 1
Identified natural frequency of the bilinear oscillator (Hz).

	Analytical	Identified results		
		Without noise	5% noise	10% noise
From global responses	22.84	22.84	22.84	22.84
From the responses $x>0$	19.49	19.49	19.45	19.45
From the responses $x<0$	27.57	27.47	27.65	27.78

The only peak is associated with the natural frequency of the associated region. The identified natural frequencies are listed in Table 1. In all tables in the paper, "Analytical" results denote results obtained by performing eigenvalue decomposition of system mass and stiffness matrices, and "Identified" results denote results extracted from simulated acceleration responses.

From Table 1, it is found that the identification accuracy is all very high under different measurement noise levels using the proposed method. However, although the identified accuracy of the bilinear frequency from the global responses is also high, the natural frequency of each region cannot be obtained from the identified bilinear frequency.

5.2. A beam with a breathing crack

This example is to illustrate the advantages of the proposed procedure for detecting breathing cracks over traditional approaches.

A cantilever beam with a single edge breathing crack, as shown in Fig. 5, was considered. Its geometry dimensions were taken as $L=1$ m, $w=0.015$ m and $b=0.050$ m. Young's modulus of $E=206$ GPa and a mass density of 7850 kg m^{-3} were assumed as material properties. The breathing crack was located near the clamped end and the distance of the crack from the free end l_c was $0.95L$.

It was assumed that the beam vibrated predominantly under its first mode. The details on the determination of parameters k_1, k_2 and m in the governing equation of motion is referred to Ref. [24]. The generalized mass and stiffness under this mode when the crack is close are obtained as

$$m = 0.228m'L, \quad k_2 = \frac{EI\pi^4}{32L^3}$$

where m' is the mass per unit length.

To get the generalized stiffness coefficient when the crack is open (k_1), the change in the flexibility due to the presence of the crack is first determined as

$$\Delta f = \frac{72l_c^2\pi(1-\nu^2)}{Ewb^4}\varphi$$

where ν is Poisson's ratio, and the function φ can be determined by

$$\varphi = 19.60\frac{a^{10}}{b^8} - 40.69\frac{a^9}{b^7} + 47.04\frac{a^8}{b^6} - 32.99\frac{a^7}{b^5} + 20.30\frac{a^6}{b^4} - 9.98\frac{a^5}{b^3} + 4.60\frac{a^4}{b^2} - 1.05\frac{a^3}{b} + 0.63a^2$$

where a is the depth of the crack. Then, the total flexibility when the crack is open is computed as

$$f_1 = f + \Delta f$$

where f is the flexibility when the crack is closed, and $f=1/k_2$. Accordingly, the stiffness when the crack is open is obtained as

$$k_1 = \frac{1}{f_1}$$

It was assumed that the beam had orthogonal viscous damping, and the damping ratio of the considered mode was 0.5%. The acceleration responses under an impact force ($x=0$, $\dot{x}=1$ m/s) were calculated by the Runge–Kutta method. To simulate the real measurement field, Gaussian white noises with a mean value of zero and a RMS of 5% of the responses were added to the acceleration responses.

Consider the intact case ($a=0$) and the following three damage cases with different crack depths, $a=0.5b$, $a=0.3b$ and $a=0.1b$, where a and b denote the depth of the crack and the beam. The procedure presented in Fig. 6 was employed to identify the breathing crack and to quantify the crack qualitatively. After obtaining the local responses corresponding to each region, the Eigenvalue Realization Algorithm (ERA) was carried out to identify the natural frequency of each region. Please note that same identification results can be obtained by simpler approaches such as peak-picking of a PSD estimation. The identified results are listed in Table 2. Compared with the analytical results obtained by eigenvalue decomposition, the natural frequencies in all cases were obtained with high accuracy. Then the difference in the natural frequency between the two regions is calculated and listed in the last column of Table 2. When the crack depth is half of

Table 2
Identified results from global responses and local responses corresponding to each region of the beam (Hz).

	ω_0 of entire system		ω_2 in region $x<0$		ω_1 in region $x\geq 0$		$\frac{\omega_{0,i}-\omega_{0,d}}{\omega_{0,i}}$	$\frac{\omega_2-\omega_1}{\omega_2}$
	Analytical	Identified	Analytical	Identified	Analytical	Identified		
$a=0$	43.00	43.00	43.00	42.71	43.00	43.32		1.42%
$a=0.5b$	39.12	39.12	43.00	42.96	35.89	36.02	9.02%	16.15%
$a=0.3b$	41.77	41.77	43.00	42.86	40.61	40.76	2.87%	4.90%
$a=0.1b$	42.86	42.86	43.00	43.06	42.72	42.66	0.33%	0.91%

the beam depth, the natural frequency of the region $x\geq 0$ (ω_1) deviates seriously from that of the region $x<0$ (ω_2) and the percentage change is 16.15%. One can easily tell that a breathing crack has occurred in this beam.

For an intermediate crack depth $a=0.3b$, the percentage change is 4.90%. Prior research has suggested that environmental factors could lead to the percentage change of up to 5% in the natural frequency even without any damage [19]. However, the percentage change of 4.90% obtained by the proposed approach can still tell that a breathing crack has occurred, because this percentage change is calculated from two sets of local response data separated from the same measured responses and thus the difference in environmental factors before and after damage has been avoided.

For comparison, a traditional approach which compares the bilinear frequencies before and after damage was also applied and the results are listed in Table 2. For each case, the bilinear frequency was identified from the global responses and then the difference between the identified bilinear frequencies before and after damage was calculated. For the case of $a=0.5b$, although the bilinear frequency before and after cracking does change, its percentage change (9.02%) is much smaller than that obtained by the proposed procedure (16.15%), which verifies the sensitivity analysis in Section 3. This trend can be observed in the other two damage cases. This means that the traditional approach could underestimate the crack depth even if it can identify presence of the crack, which might be very dangerous. For the intermediate crack depth $a=0.3b$, the traditional approach failed to identify the presence of the crack due to the small percentage change. In addition, the baseline data is required in the traditional approach. However, the baseline data may be difficult to obtain in most practical applications.

For the case with a smaller crack depth $a=0.1b$, although the percentage change in the natural frequency between two regions is much greater than the percentage change in the bilinear frequency before and after damage, it is difficult to tell that a crack occurs using the proposed procedure. This is because the identification error may be greater than the percentage change in natural frequencies between the two regions (0.91%) caused by the breathing crack. Actually, the crack with this depth just introduced the stiffness reduction of 1.31%. The traditional approach was not able to identify this small crack either.

As can be seen from Table 2, the percentage change in the natural frequencies between the two regions decreases monotonically as the crack depth decreases, which suggests that the proposed procedure can provide a qualitative indication of crack size. The greater the difference, the more severe the crack.

5.3. A beam with a large deflection

This example is to investigate the performance of the proposed procedure for detecting fatigue cracks for systems which are nonlinear in each region, i.e., piecewise-nonlinear systems.

Consider the same beam as used in Section 5.2 except that a concentrated mass of (100–1.34 kg, herein 1.34 kg is the self-weight of the beam) was added at the free end. The concentrated mass induced the beam to produce a large deflection, introducing cubic stiffness nonlinearity into the beam. The motion of the beam under the first mode can be governed by Eq. (11). Assume that the coefficient of cubic stiffness in each stiffness region was 10% of the linear stiffness of the intact beam, and the damping ratio of the considered mode was 1%. Gaussian white noises with the mean value of zero and the RMS of 5% of the responses were added to the calculated acceleration responses.

Due to a large deflection, the intact beam exhibited cubic stiffness nonlinearity. Once a breathing crack occurred, the beam exhibited the characteristics of both the bilinearity and cubic stiffness nonlinearity, to be more precise, piecewise-nonlinearity.

Assume that the breathing crack occurred at the same location as in Section 5.2. The intact case and the same damaged cases ($a=0.5b$, $a=0.3b$ and $a=0.1b$) studied in Section 5.2 were considered here. The acceleration responses under an impact excitation ($x=0,\dot{x}=300\ m/s$) in each case were calculated using the Runge–Kutta method.

For the intact case, a Hilbert transform was first performed on the global responses and two sets of local responses. The three graphs in Fig. 10 represent the extracted IFs. In each figure, it is observed that: (1) due to the existence of cubic nonlinearity, the graphs of the IF decrease with time; (2) the graphs of the IFs are smooth. Then, to get a good estimation of frequency, the average of IFs between Second 12 and Second 18 in the global responses was calculated to estimate ω_0; and the average of IFs between Second 6 and Second 9 in each set of local response data was calculated to estimate ω_1 or ω_2. Because a crack does not exist in this case, the estimated ω_1 and ω_2 data are equal, which can be reflected from the middle and bottom graphs in Fig. 10. In addition, the estimated ω_1 and ω_2 are equal to the estimated ω_0.

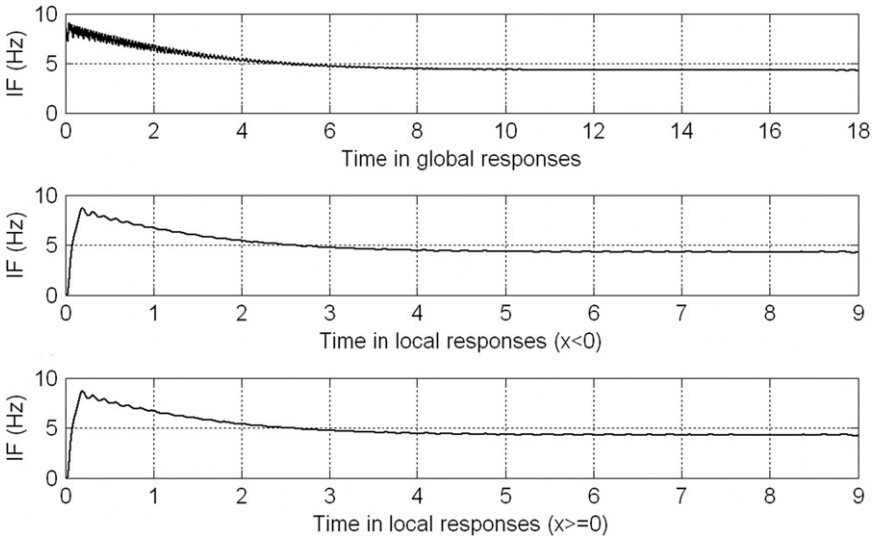

Fig. 10. Instantaneous frequency (IF) for the intact beam.

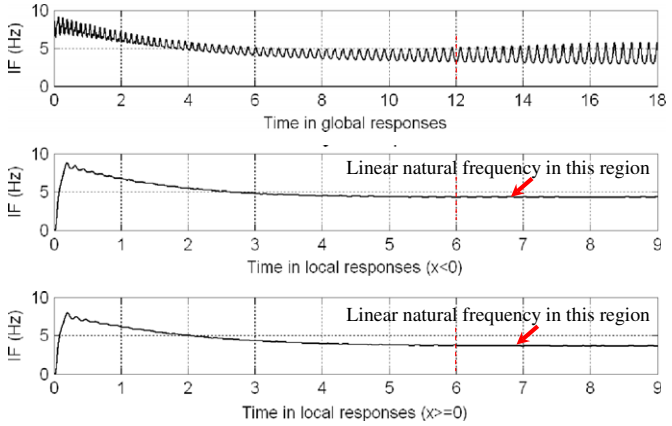

Fig. 11. Instantaneous frequency (IF) for the beam with a breathing crack ($a=0.5b$).

The same procedure was applied to the damage case $a=0.5b$. The upper graph in Fig. 11 represents the IFs extracted from the global responses. It is observed that the IF not only decreases with time, but also oscillates with time, unlike the smooth graph in Fig. 10 associated with the uncracked beam. Actually, the decreasing trend of the IF is caused by the cubic stiffness nonlinearity, and the oscillation trend is caused by the bilinear stiffness nonlinearity. The linear stiffness varies from one region to the other region periodically, and accordingly the natural frequency of the underlying linear system varies periodically, which is why oscillations exist in the IF graph even at the end of the decaying vibration. Actually, the greater the variation in the linear stiffness, the stronger the bilinearity, and the larger the oscillation amplitude in the IF graph. In the upper graph, the average of the IF towards the end of the decaying vibration (between Second 12 and Second 18) was obtained as the estimation of the bilinear frequency.

The middle and bottom graphs in Fig. 11 represent the IFs extracted from each set of local response data. It can be seen that only the decreasing trend of IFs exists and the oscillation trend of IFs does not exist. This is because each set of local response data includes only the information on the cubic stiffness nonlinearity of each region. The average of the IFs between Second 6 and Second 9 was calculated to obtain the estimate of the natural frequency of the underlying system in each region, ω_1 or ω_2, as listed in Table 3.

For the other two cases, ω_1 and ω_2 were obtained in the same way, and are listed in Table 3. The percentage change of the natural frequency between the two regions is listed in the last column for each case. For comparison, the change in the bilinear frequency between the intact beam and the cracked beam is also listed. Similar results to the example in Section 5.2 were obtained. The proposed procedure was able to identify the two damage cases, $a=0.5b$ and $a=0.3b$ and to provide a qualitative indication of crack depth. However, only the severe crack $a=0.5b$ was identified using the traditional bilinear frequency-based method.

Table 3
Identified results from global responses and local responses corresponding to each region of the beam with a large deflection (Hz).

	ω_0 of entire system		ω_2 in region $x<0$		ω_1 in region $x\geq 0$		$\frac{\omega_{0,i}-\omega_{0,d}}{\omega_{0,i}}$ (%)	$\frac{\omega_2-\omega_1}{\omega_2}$ (%)
	Analytical	Identified	Analytical	Identified	Analytical	Identified		
$a=0$	4.30	4.30	4.30	4.30	4.30	4.31		0.00
$a=0.5b$	3.91	3.93	4.30	4.31	3.59	3.60	8.60	16.35
$a=0.3b$	4.18	4.18	4.30	4.30	4.06	4.07	2.94	5.34
$a=0.1b$	4.29	4.29	4.30	4.30	4.27	4.27	0.34	0.70

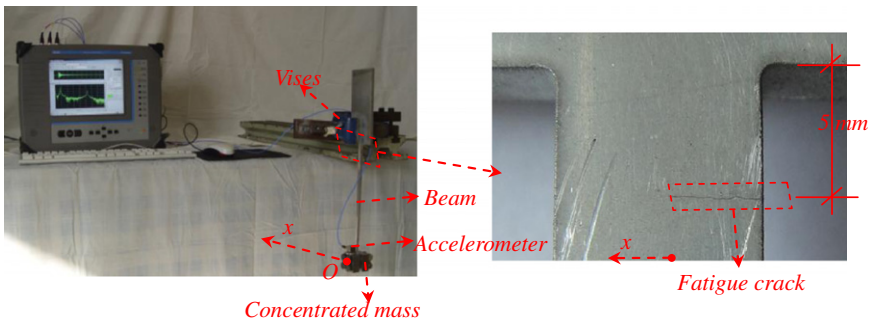

Fig. 12. Experimental setup and simulated damage scenario.

6. Experimental validation

6.1. Experimental setup

The proposed procedure for detecting fatigue cracks was further validated by experimental tests on a cantilever beam with a fatigue crack, as shown in Fig. 12. The beam is 275 mm long, 8 mm wide and 4 mm thick. It was made of aluminum (7075-T651). A concentrated mass of 0.5 kg was mounted at the free end. The beam was clamped at the upper end to ensure that the stiffness interface in the restoring force model is at $x=0$.

The fatigue crack on the beam was simulated as a single crack through the thickness, as shown in Fig. 12. The crack was located 5 mm away from the clamped end. The tested beam was machined from a big piece of aluminum plate with a fatigue crack produced by Professor Alten F. Grandt at Purdue University. Details on making the fatigue crack can be found in Chapter 3 of Ref. [25].

An accelerometer (PCB three-axial *M356A25*) was deployed at the free end of the cantilever beam to measure the acceleration responses in the horizontal (x) direction, as shown in Fig. 12. Free-vibration responses can be generated by either an initial displacement at the free end or by exciting the beam at the free end using a sinusoidal signal with a frequency close to the first natural frequency of the beam for a while and then stopping the excitation. Herein, an initial displacement was employed. The *COMPASS* dynamic signal analyzer (*Nicolet*) was used to acquire acceleration responses at a sampling frequency of 160 Hz. The acquisition duration was 50 s.

6.2. Finite element model

The finite element models of the uncracked and cracked beams were developed using MATLAB and modal analysis was performed to obtain the analytical natural frequencies, as listed in the 2nd and 3rd rows of Table 4. In addition, the percentage change of the bilinear frequency before and after damage was calculated to be 6.29%, which is much smaller than the percentage change in the natural frequency between the two regions (11.30%).

6.3. Results and discussions

The measured acceleration responses are plotted in Fig. 13. It can be observed that: (1) the global responses are not symmetrical about the axis of *acceleration*$=0$, which is the consequence of the existence of bilinearity; (2) the response curve is not smooth, which could be caused by measurement noises. Table 4 lists the bilinear frequency identified by performing Fourier transform on the measured global responses. The identified result, 8.79 Hz, matches that obtained from the finite element analysis.

Before performing the proposed procedure for detecting the fatigue crack, a short-time Fourier transform was performed on the measured responses to identify the range of responses to be used for further analysis. The obtained

Table 4
Natural frequencies of experimental specimen (Hz).

	ω_0 of entire system	ω_2 in region $x<0$	ω_1 In region $x\geq 0$	$\frac{\omega_2-\omega_1}{\omega_1}$ (%)
Analytical $a=0$	9.47	9.47	9.47	0.00
Analytical $a=0.5b$	8.91	9.47	8.40	11.30
Experimental $a=0.5b$	8.79	9.38	8.30	11.49

Note: a and b denote the depth of the crack and the depth of the beam, respectively.

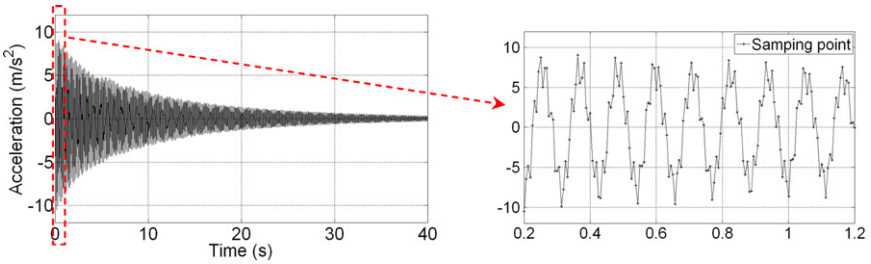

Fig. 13. Measured acceleration responses.

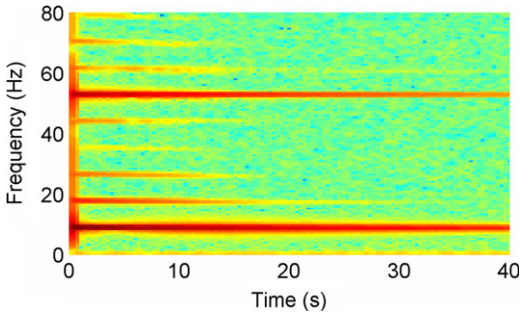

Fig. 14. Time–frequency diagram of measured responses.

time–frequency diagram is plotted in Fig. 14. It can be seen that: (1) the fundamental bilinear frequency is 8.79 Hz; (2) the higher harmonics of 8.79 Hz exist (please note that the frequency component of about 55 Hz could be caused by electric current). However, the higher harmonics decay very quickly with the decay of responses. It suggests that the crack stopped opening and no bilinearity was involved in the system when the responses were small. Therefore, the fatigue crack can only be captured in the first few seconds of response data which involves the bilinearity information. Herein, the first five seconds of response data was used for further analysis.

Before separating the selected range of responses to obtain local responses, interpolation was performed to ensure the separation points to be as close to the axis of *acceleration*$=0$ as possible. The sampling frequency of the interpolated data was 10 times the original sampling frequency 160 Hz, which was 1600 Hz. Then the interpolated data was divided at $x=0$ and put together to form two sets of local response data, which are plotted in Fig. 15. It is worth noting that the signs of acceleration and displacement are opposite, and thus positive acceleration responses are associated with the region $x<0$, and vice versa.

By performing Fourier transform on the two sets of local response data respectively, the natural frequency of each region can be obtained. The graphs of power spectral density of the two sets of local response data are plotted in Fig. 16. The peak of the red dashed graph is 16.60 Hz, which is twice the natural frequency of the region $x\geq 0$, giving the natural frequency of 8.30 Hz for the associated region. Likewise, the peak of the black graph gives the natural frequency of the other region, 9.38 Hz. The percentage change of the natural frequencies between the two regions is 11.49%, which matches the analytical results quite well. In addition, the bilinear frequency calculated from the identified natural frequency of each region using Eq. (4) is 8.80 Hz, matching the natural frequency extracted from the global response data 8.79 Hz. The identified natural frequencies are listed in the 4th row of Table 4. From the difference in the natural frequency between two regions 11.49%, we can easily tell that a fatigue crack has taken place on the beam without knowing the baseline data.

7. Conclusions

An approach to detecting breathing-fatigue cracks was developed based on dynamic characteristics of breathing cracks. This method offers a simple but effective technique for practical engineering structures. First, a system identification

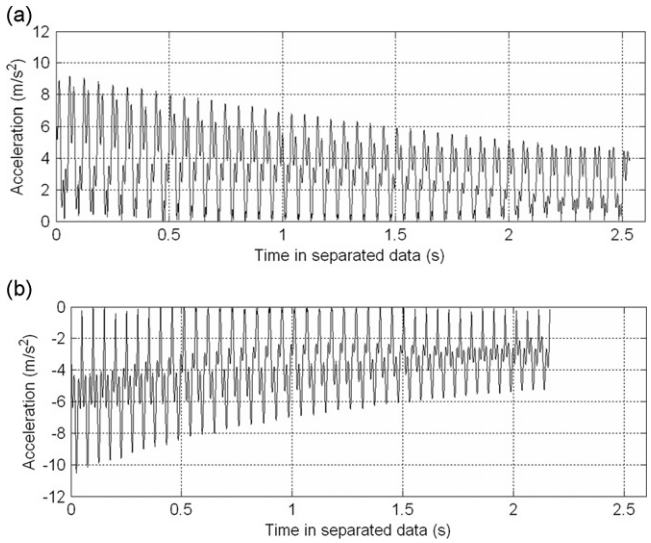

Fig. 15. Local responses separated from global responses: (a) local responses associated with the region $x < 0$ and (b) local responses associated with the region $x \geq 0$.

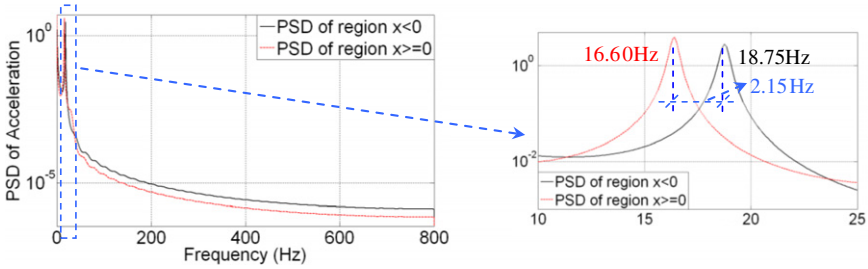

Fig. 16. Power spectral density of two sets of local response data. (For interpretation of the references to color in this figure legend, the reader is referred to the web version of this article.)

method for bilinear systems was proposed by separating impulse or free-vibration responses of the system into local responses corresponding to each stiffness region. This method transfers nonlinear system identification into linear system identification. Then, the procedure for identifying the existence of breathing cracks and quantifying the cracks qualitatively was proposed by comparing the natural frequencies extracted from each set of local responses. Finally, by introducing Hilbert transform, the proposed procedure was extended to identify breathing cracks in piecewise-nonlinear systems. Only either acceleration or displacement responses are required to be measured.

The results from numerical simulations and experimental tests have shown that the proposed approach to detecting fatigue cracks offers the following advantages over traditional approaches that are based on the bilinear frequency: (1) this approach is more sensitive to breathing cracks than traditional approaches; (2) it does not require the baseline data, because this approach compares the natural frequencies of different stiffness regions which are extracted from the responses separated from the same global responses measured in the current state; (3) it is not affected by the difference in measuring environmental factors, boundary conditions or measurement errors in different measurements, because the natural frequencies of each region are obtained from the same responses measured at one time. Therefore, the proposed approach is more reliable and effective for crack detection than traditional methods.

Because the proposed approach takes advantage of dynamic characteristics of breathing cracks, if a fatigue crack does not breathe (always open), the proposed approach will fail to detect this fatigue crack. In this case, the baseline data is required and damage can be identified using approaches proposed for detecting unbreathing cracks, for example, by comparing the current natural frequencies and the baseline natural frequencies.

For breathing-fatigue cracks, the proposed approach will work well when the external excitation (dynamic loadings) acting on the structure can be controlled. In some practical applications, however, no such controllable excitation is permitted and only operational/ambient excitation is applied. In this situation, two cases are worth being discussed: (1) if the operational/ambient excitation is not either a sinusoidal excitation with a frequency close to a natural frequency of the structure in question or a broad-band random excitation, it may not be able to excite any natural frequency of the structure. Then the natural frequencies in each region cannot be identified, which can render the proposed approach to fail to detect fatigue cracks; (2) if the operational/ambient excitation is a broad-band random excitation, several natural

frequencies of the structure can be excited. After separating the global responses into local responses, several natural frequencies can be extracted from each set of local responses. The natural frequencies with the same order extracted from a different set of local responses will be different if breathing cracks exist, which indicates the presence of fatigue cracks. The validation and possible improvement of the present approach for use in this kind of application will be the objective of future work.

Acknowledgments

The authors would like to express their sincere gratitude and appreciation to Professor Keith Worden at the University of Sheffield for discussions and invaluable advice and suggestions. The authors wish to address special thanks to Professor Alten F. Grandt in School of Aeronautics and Astronautics at Purdue University for providing the experimental specimen. In addition, the authors would like to Professor Liangrao Tu and Mr. Jianxin Yu at Harbin Institute of Technology for helping carry out the experimental tests. Furthermore, this study has been financially supported by the RELUIS Project, "Health Monitoring of Deep Tunnel", and the National Natural Science Foundation of China under Grant no. 50708029, which are gratefully appreciated. Last but not least, the authors would like to thank the two anonymous reviewers for their valuable comments which are very important for the authors to improve this paper.

References

[1] T.G. Chondros, A.D. Dimarogonas, J. Yao, Vibration of a beam with a breathing crack, *Journal of Sound and Vibration* 239 (2001) 57–67.
[2] G.-L. Qian, S.-N. Gu, J.-S. Jiang, The dynamic behaviour and crack detection of a beam with a crack, *Journal of Sound and Vibration* 138 (1990) 233–243 .
[3] Y.C. Chu, M.-H.H. Shen, Analysis of forced bilinear oscillators and the application to cracked beam dynamics, *AIAA Journal* 30 (1992) 2512–2519.
[4] K. Worden, G.R. Tomlinson, *Nonlinearity in Structural Dynamics: Detection, Identification and Modelling*, Institute of Physics Publishing, Bristol and Philadelphia, 2001, pp. 299–300.
[5] W.H. Leong, W.J. Staszewski, B.C. Lee, F. Scarpa, Structural health monitoring using scanning laser vibrometry: III. Lamb waves for fatigue crack detection, *Smart Materials and Structures* 14 (6) (2005) 1387–1395.
[6] Jeong-Beom Ihn, Fu-Kuo Chang, Detection and monitoring of hidden fatigue crack growth using a built-in piezoelectric sensor/actuator networ: I. Diganostics, *Smart Materials and Structures* 13 (3) (2004) 609–620.
[7] Q. Shan, R.J. Dewhurst, Surface-beaking fatigue crack detection using laser ultrasound, *Applied Physics Letters* 62 (21) (1993) 2649–2651.
[8] T.M. Roberts, M. Talebzadeh, Acoustic emission monitoring of fatigue crack propagation, *Journal of Constructional Steel Research* 59 (6) (2003) 695–712.
[9] S.L. Tsyfansky, V.I. Beresnevich, Detection of fatigue cracks in flexible geometrically non-linear bars by vibration monitoring, *Journal of Sound and Vibration* 213 (1998) 159–168.
[10] A.P. Bovsunovskya, C. Surace, Considerations regarding superharmonic vibrations of a cracked beam and the variation in damping caused by the presence of the crack, *Journal of Sound and Vibration* 288 (2005) 865–886.
[11] Jacques Francois Leonard, Serge Lanteigne, Lalonde, Yvon Turcotte, Free-vibration behaviour of a cracked conatilever beam and crack detection, *Mechanical Systems and Signal Processing* 15 (3) (2001) 529–548.
[12] A. Rivola, P.R. White, Bispectral analysis of the bilinear oscillator with application to the detection of fatigue cracks, *Journal of Sound and Vibration* 216 (1998) 889–910.
[13] Cecilia Surace, Romualdo Ruotolo, David Storer, Detecting nonlinear behavior using Volterra series to assess damage in beam-like structures, *Journal of Theoretical and Applied Mechanics* 49 (3) (2011) 905–926.
[14] S. Loutridis, E. Douka, L.J. Hadjileontiadis, Forced vibration behaviour and crack detection of cracked beams using instantaneous frequency, *NDT&E International* 38 (2005) 411–419.
[15] J. Ryue, P.R. White, The detection of cracks in beams using chaotic excitations, *Journal of Sound and Vibration* 307 (2007) 627–638.
[16] P. Gudmundson, The dynamic behaviour of slender structures with cross-sectional cracks, *Journal of the Mechanics and Physics of Solids* 31 (1983) 329–345.
[17] A. Ibrahim, F. Ismail, H.R. Martin, Modelling of the dynamics of a continuous beam including nonlinear fatigue crack, *Journal of Modal Analysis* 2 (1987) 76–82.
[18] P.V. Bayly, On the spectral signature of weakly bilinear oscillators, *Journal of Vibration and Acoustics* 118 (1996) 352–361.
[19] Charles R. Farrar, Keith Worden, Michael D. Todd, Gyuhae Park, Jonathon Nichols, Douglas E. Adams, Matthew T. Bement, Kevin Farinholt, Nonlinear System Identification for Damage Detection, LA-14353-MS, November 2007.
[20] R.W. Clough, Joseph Penzien, *Dynamics of Structures*, Computers and Structures, Inc., 2003.
[21] B. Peeters, J. Maeck, G.D. Roeck, Vibration-based damage detection in civil engineering: excitation sources and temperatures effects, *Smart Materials and Structures* 10 (2001) 518–527.
[22] Guirong Yan, A.D. Stefano, B. Uy, G. Ou, X.Q. Zhu, A general nonlinear system identification method based upon the time-varying trend of the instantaneous vibration frequency and amplitude, *Advances in Structural Engineering* 15 (2012) 781–792.
[23] M.G. Sainsbury, Y.K. Ho, Application of the time domain fourier filter output (TDFFO) method to the identification of a lightly damped non-linear system with an odd-spring characteristic, *Mechanical Systems and Signal Processing* 15 (2001) 357–366.
[24] S.M. Cheng, X.J. Wu, W. Wallace, Vibrational response of a beam with a breathing crack, *Journal of Sound and Vibration* 225 (1999) 201–208.
[25] Matthew David Gates, A Crack Gage Approach to Monitoring Fatigue Damage Potential in Aircraft, Master Thesis, Aeronautical and Astronautical Engineering, Purdue Univeristy, May 1997 (Supervised by Alten F. Grandt, Jr.).